Carbohydrate Polymers **14** (1991) 17–27

Conformational Aspects of Xanthan–Galactomannan Gelation. Further Evidence from Optical-Rotation Studies

Norman W. H. Cheetham & Ernest N. M. Mashimba

School of Chemistry, The University of New South Wales, PO Box 1, Kensington, New South Wales 2033, Australia

(Received 17 July 1989; revised version received 24 September 1989; accepted 30 September 1989)

ABSTRACT

Optical-rotation versus temperature profiles have been used to probe some aspects of the mechanism of gel formation between xanthan gum and locust bean (carob) gum.

Evidence is presented which further strengthens the proposal that intermolecular associations to form gel junction zones occur with the xanthan in the disordered conformation rather than in the ordered, helical structure. Results for gelation in water and in 0·05 M potassium chloride solution are discussed.

INTRODUCTION

When solutions of galactomannans such as locust bean gum (LBG) are mixed with xanthan gum solutions, gelling may occur. The nature of the mixed xanthan/LBG junction zones is of interest here. The conformation of each polysaccharide involved in a junction zone is a point of some debate. There seems to be general agreement that the LBG is in a twofold ribbon of conformation, i.e. the mannan backbone is in a cellulose-like form. Opinions differ as to the conformation of the xanthan. Morris *et al.* (1977) and Dea *et al.* (1977) propose the ordered, helical conformation for xanthan in junction zones. Cairns *et al.* (1986, 1987) proposed a different model based on X-ray fibre-diffraction studies on stretched gels, which indicate a repeat distance of 0·52 mm. Cairns *et al.* interpret these results by way of

Carbohydrate Polymers 0144-8617/90/$03.50

(a) A sandwich model for the mixed xanthan/LBG/xanthan junction zones. Side chains of the xanthan molecules on either side of the galactomannan are staggered, resulting in a 50% displacement between the two xanthan backbones such that the repeat distance in the X-ray fibre-diffraction patterns is 0·52 nm. As pointed out by Cairns *et al.* (1987), such a sandwich structure (which could grow in the b & c-dimensions but would have limited periodicity in the a-dimension) should show streaking of reflections on all layer lines. This was not observed experimentally.

(b) A random co-crystallisation of xanthan and galactomannan, with the large trisaccharide side chains of xanthan acting as defects in the a-dimension. 'The mixed-gel diffraction patterns are equivalent to pure galactomannan patterns for which only Okl reflections are allowed', Cairns *et al.* (1987). This was suggested as a more likely model, but still leaves unanswered the reasons for the sensitivity of xanthan/galactomannan interactions to both the mannose/galactose (M/G) ratio *and* the fine structure of the galactomannan. Some observations which help to explain the observed effect of galactomannan fine structure on gel strength are more fully discussed in a previous paper (Cheetham & Mashimba, 1988). That paper provided gel melting point and optical-rotation data to support the proposal that xanthan in mixed xanthan/LBG junction zones was in the disordered conformation, probably with the backbone in the twofold ribbon conformation. This paper presents further optical-rotation evidence that the disordered form of xanthan is involved in such junction-zone formation.

EXPERIMENTAL

The origin and preparation of xanthan gum samples and solutions have been described previously (Cheetham & Mashimba, 1988). Solutions for optical-rotation studies were filtered through a 1·2-μm membrane. Locust bean gum (LBG-E; Mw 144×10^3, M/G ratio 5·2) was obtained by β-D-mannanase treatment of hot-water-soluble LBG, as previously described (Cheetham *et al.*, 1986). Acetate and pyruvate were determined by HPLC, as described by Cheetham and Punruckvong (1985). Optical rotations were measured at 365 nm in a Perkin-Elmer 141 polarimeter, using a 1-ml, thermostatted, quartz cell (path length 10 cm). The cell temperature was raised from ambient to 90°C at 1·5°C/min, by a

Julabo VC-5 circulating waterbath and Model PRG-1 programmer. Cooling to room temperature was achieved by switching off the waterbath heating element. Typically, cooling time was 6 h. Final concentrations of clarified xanthan and LBG solutions were determined by the phenol/sulphuric acid procedure (Dubois *et al.*, 1956), using the respective polysaccharides as standards.

RESULTS AND DISCUSSION

Experiments were carried out on semi-dilute solutions ($\approx 0{\cdot}25\%$ total polysaccharide) in water or in 0·05 M KCl. These conditions permitted the xanthan order/disorder transition to be observed by polarimetry. Though some experiments were performed under gel-forming conditions, the low-Mw LBG-E combined with the 0·25% total polysaccharide level avoided this complication. In early experiments, higher concentrations and larger LBG samples caused problems. It has been shown (Cheetham & Punruckvong, 1989) that xanthan/LBG interactions still occur with the lower-Mw polysaccharide samples. As concentration and ionic strength strongly influence certain xanthan properties, it is important that the conditions used herein be borne in mind. Figure 1 shows the optical-rotation versus temperature profiles for xanthan in 0·05 M KCl solution. The heating and cooling curves are significant. In salt, xanthan alone has a specific optical-rotation versus temperature profile ranging from ≈ -44 to $\approx -27°$. The cooling curve is almost identical to the heating curve. The large, negative initial rotation indicates that the xanthan chains were largely in the ordered, helical conformation. Heating yields the typical sigmoidal curve associated with the well documented order/disorder transition of xanthan. The midpoint temperature of this transition (T_c) is characteristic of a particular sample, and is also dependent on factors such as salt concentration, pyruvate content, and the presence of other polysaccharides, such as galactomannans. On cooling, the xanthan in salt returns immediately to the ordered conformation with little evidence of hysteresis. This has been observed previously (Norton *et al.*, 1984; Richardson & Ross-Murphy, 1987). Slight differences between the initial and final optical rotation of most samples in salt were observed. The magnitude of these differences are approaching the order of experimental error for the Perkin-Elmer 141 polarimeter, and are thus not given great emphasis here. The final rotation after a heat/cool cycle is nearly always less negative than the initial rotation. The initial rotation is not restored even on storing for up to 5 days. We believe the effect to be real, and tentat-

ively attribute it to rearrangement of the initial intermolecular associations between xanthan chains. These associations are disrupted upon heating, and on cooling are re-established in a slightly modified form.

The precise nature of xanthan/xanthan intermolecular associations is not known. Possibilities include concentric double helices over limited regions, perhaps involving only limited portions near the chain ends, and side-by-side helices. Side-chain/side-chain associations involving pyruvate methyl groups could be involved in stabilising the latter forms (Smith *et al.*, 1981; Frangou *et al.*, 1982). Such associations are enhanced in salt. Whatever their nature, the intermolecular associations are believed to be important contributors to the unusual rheological properties of xanthan solutions (Frangou *et al.*, 1982).

The situation in water is different (Fig. 2). The initial specific rotation of xanthan samples in water is always less negative than in salt. The actual value depends on the history of the xanthan and on how thoroughly it was dialysed. Cheetham and Mashimba (1988) and others (Lecourtier *et al.*, 1986; Milas & Rinaudo, 1986) have shown that dialysis of xanthan against water results in an upward shift in optical rotation towards that of the disordered state. The final rotation depends on the extent of dialysis and on the pyruvate content of the sample. High-pyruvate samples, after exhaustive dialysis (to constant conductivity), have optical rotations not greatly different from those of the disordered form of xanthan observed in water at temperatures above ≈ 50°C (Fig. 2).

In water, electrostatic repulsions involving glucuronate and pyruvate in the side chains are poorly shielded, favouring the disordered conformation. The specific optical rotation of a particular sample in water is thus always more positive than that in salt solution.

Consequently, the specific optical rotation should be an overall indicator of xanthan conformation. Figure 2(a) shows the results of heating a partially dialysed xanthan sample. The cooling curve, Fig. 2(b), shows a marked departure from the heating curve. Cooling from 90 to 25°C was allowed to take place over several hours. On further standing (≈ 1 day) the optical rotation returned to be very close to the original reading. Figure 2(c and d) shows the heating and cooling curves, respectively, for an exhaustively dialysed sample, which on longer standing also returned to the initial rotation. Solutions of xanthan in water thus take much longer than solutions in salt to recover their initial conformation, after being subjected to an order/disorder treatment. Figure 3(a) shows the heating curve for an optical-rotation experiment in water, using a partially dialysed xanthan sample. Figure 3(b) shows the curve for the same xanthan sample in the presence of LBG. The conformation and

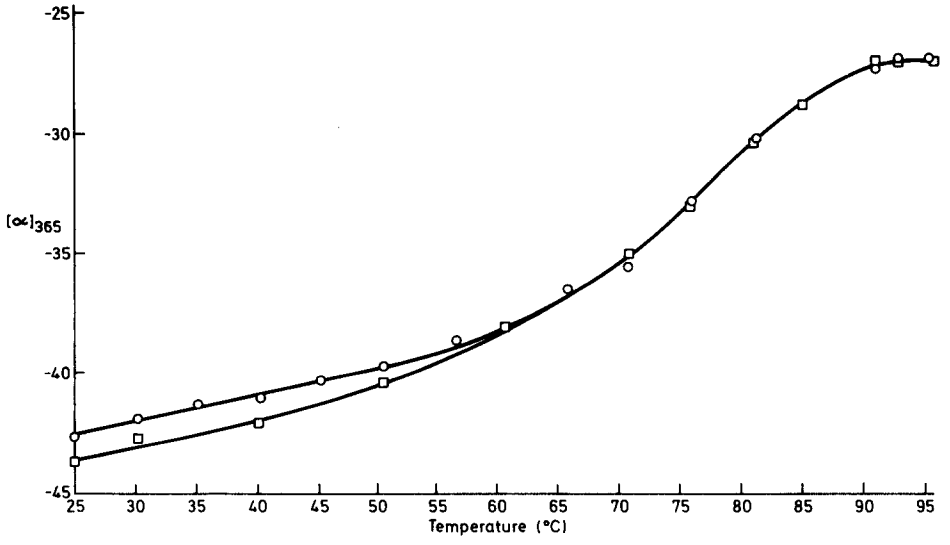

Fig. 1. Optical-rotation versus temperature profile for xanthan (0·25%) in 0·05 M KCl solution; □ heating, ○ cooling.

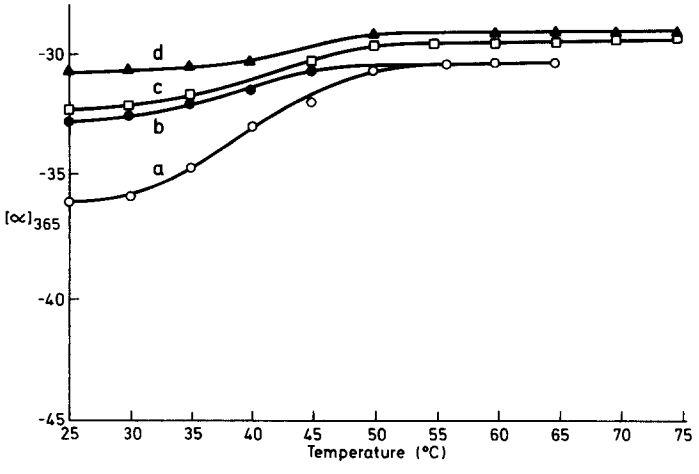

Fig. 2. Optical-rotation versus temperature profiles for xanthan (0·25%) in water. (a) Partially dialysed xanthan, heating; (b) partially dialysed xanthan, cooling; (c) exhaustively dialysed xanthan, heating; (d) exhaustively dialysed xanthan, cooling.

molecular weights of the polysaccharides are such that actual gel formation at 25°C does not occur. This avoids the complications of gel strain effects on the optical-rotation experiment. It has been shown that such a system constitutes a valid model for gel formation, as the same xanthan/LBG interactions occur (Cheetham & Punruckvong, 1989).

The optical-rotation value of LBG alone over the range of the experiment was essentially constant, and this value has been substracted from the values of a xanthan/LBG mixture to yield the curve in Fig. 3(b). The initial (i.e. prior to heating) optical rotation of the xanthan/LBG mixture in Fig. 3(b) is significantly less negative than that of xanthan alone. The final optical rotation, i.e. above $\approx 60°C$, is identical to that of xanthan alone. We interpret this to mean that in the presence of LBG, (i.e. under gel-forming conditions) xanthan at room temperature is induced to take up, in the (limited) junction-zone regions at least, the disordered conformation (as indicated by the upward shift in optical rotation). These results have been carefully confirmed in a number of cases. On cooling, Fig. 3(c), a curve similar to that observed with xanthan alone, Fig. 2(a and b), occurs. Thus, cooling to 25°C (gel-forming conditions) apparently leaves the xanthan with an even greater amount of the disordered conformation than before heating. A tentative conclusion is that junction-zone formation occurs with xanthan in the disordered conformation. However, as xanthan alone shows a similar curve to that in Fig 3(b and c), a further observation proved crucial. The final (25°) optical rotation observed in Fig. 3(c) was maintained, on prolonged storage, in contrast to those in Fig. 2(b and d). It was maintained even after refrigeration. The xanthan/LBG junction zones apparently 'locked' the polysaccharide chains in their appropriate conformations. The chain regions not involved in junction-zone formation (probably a major part of each chain, as junction zones are limited in size) are, on cooling, largely constrained by the network of junction zones from returning to the more ordered conformation. In the absence of salt then, the overall, specific optical rotation is approximately $-31°$.

In the presence of salt, an analogous situation is observed. Figure 4(a) shows the optical-rotation versus temperature profile for xanthan alone in 0·05 M KCl solution. Figure 4(b) shows the heating profile of the same sample in the presence of LBG. As in Fig. 3(b), the initial optical rotation is less negative than that of xanthan alone, though to less an extent ($\approx 2°$ *cf* 5°). The situation in Fig. 4(b) corresponds to gel-island formation by full-sized molecules (Cheetham & Mashimba, 1988). Smaller regions of the xanthan have been induced into a more disordered conformation (as the ordered conformation is stabilised by the KCl) and form junction zones with LBG.

Figure 4(c) shows the second heating cycle for the same sample. (The initial optical rotation is above that of Fig. 4(b) as it corresponds to the bottom of the first cooling cycle.) Figure 4(d and e) show the third-heating and cooling cycles, respectively, after which further heating and cooling cycles are identical. The final optical-rotation reading (corresponding to

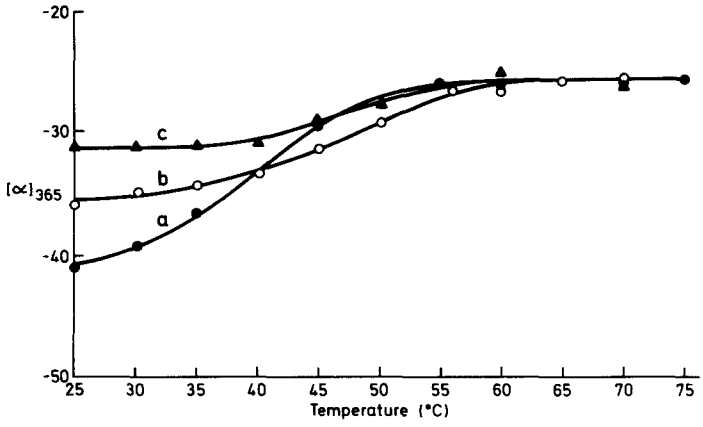

Fig. 3. Optical-rotation versus temperature profiles for xanthan (0·25%) in water. (a) Partially dialysed xanthan, heating. (b) Partially dialysed xanthan + 0·25% LBG (1/1, v/v); heating. (Effect of LBG has been substracted; see text.) (c) Sample as for (b), cooling.

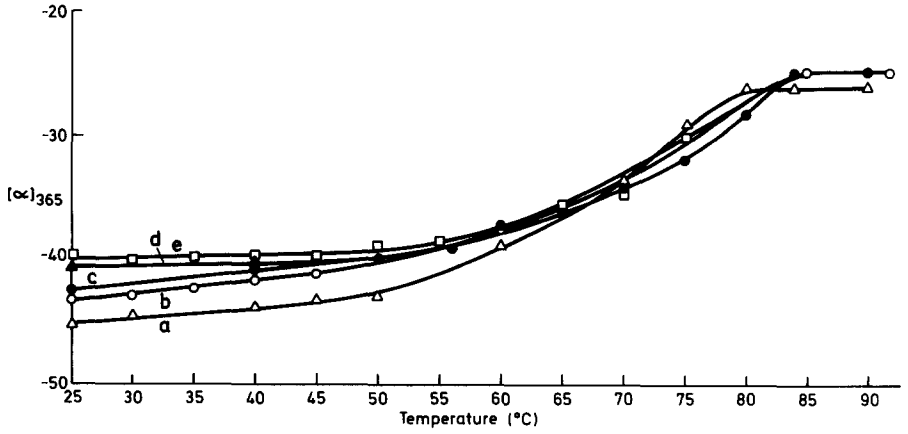

Fig. 4. Optical-rotation versus temperature profiles for xanthan 0·25% in 0·05 M KCl solution. (a) Xanthan alone, heating. (b) Xanthan + 0·25% LBG (1/1, v/v); heating, first cycle. (c) As for (b); heating, second cycle. (d) As for (c); heating, third cycle. (e) As for (d); cooling curve.

the formation of a strong gel by full-sized molecules) is about 5° less negative than the initial (pre-heating) reading. Again it is concluded that xanthan involved in junction-zone formation is in the disordered form. Prolonged standing, and even cooling, does not lower the final rotation below that in Fig. 4(e). The final optical rotation in salt is about 8° more negative than in water. The presence of salt during the cooling process,

when junction zones are being established, is a contributing factor to this. Chain regions not involved in junction zones tend to adopt the ordered conformation rapidly on cooling. The system is more complex than in water and this seems to be reflected in the number of heat/cool cycles needed before a constant optical rotation is finally reached.

CONCLUSIONS

Changes in the ψ and ϕ conformational angles across each of the five glycosidic linkages are possible, in principle, when the xanthan molecule undergoes an order/disorder transition. Optical rotation alone cannot distinguish between changes in the individual conformational angles in the xanthan repeat unit. One conformational change involves the cellulose-like xanthan backbone. In the ordered conformation, a 5/1 helix has been proposed (Moorhouse *et al.* 1977). The order/disorder transition must, among others, bring about changes in the cellulosic ψ and ϕ angles to bring the glucose residues (on average) closer to the twofold 'ribbon' conformation of cellulose itself. Changes in the glycosidic conformational angles of the side chain units are also likely. Indeed, space-filling model-building experiments show that for the 5/1 helix to twofold ribbon transition, the side chains must swing considerably away from their original positions close to the main chain and adopt an almost vertical position (taking the backbone as horizontal), as shown in Fig. 5. A galactomannan chain, sited above the xanthan backbone and parallel to it, can stack neatly as shown in Fig.5, with any 6-*O*-α-D-galactopyranosyl units occurring on the 'rear' edge opposite the xanthan side chains. Possible hydrogen bonds between OH-3 of the galactomannan and OH-4 of the inner mannose of the xanthan side chain are shown. Also possible, on the rear edge of the chains, are hydrogen bonds involving OH-6 of the mannan backbone and OH-2 of the xanthan backbone. With the polymer chains arranged as shown, any α-1$\rightarrow$6-linked galactosyl residue on the galactomannan rear edge (dotted, broken circles) will occur almost exactly opposite the lower xanthan side chain. As a result, another xanthan molecule sited above the galactomannan and running anti-parallel to the first, is forced to have its side chains staggered (and on the opposite side) relative to those of the lower xanthan chain. Hydrogen bonds appear possible between the (unsubstituted) OH-6 on the rear edge of the mannan backbone, and OH-2 of the upper xanthan backbone chain. The models also show that substantial regions of the xanthan and LBG 'contact' surfaces consist of hydrogen atoms linked to carbon. These regions are likely to be involved

in hydrophobic interactions, which would further increase junction-zone stability, especially in salt. Figure 5 also shows the possible origin of the observed (Cairns *et al.*, 1987) X-ray diffraction 0·52-nm repeat distance for mixed xanthan/galactomannan junction zones. It was not possible to build a satisfactory junction-zone space-filling model involving the ordered, 5/1, helical conformation of xanthan, and the galactomannan chain.

Thus, the features of a possible sandwich model for xanthan/galactomannan junction zones (Cheetham & Mashimba, 1988) are maintained in Fig. 5. The necessity for the disordered conformation to be involved explains why exhaustively dialysed xanthan in water gels immediately with LBG. The arrangement in Fig. 5 is admittedly speculative, and the staggering of side chains is required for a sandwich model only.

When xanthan and LBG solutions in KCl are mixed, gel islands form initially, and only after heating above T_c does a homogeneous gel form. (Cheetham & Mashimba, 1988; Cairns *et al.*, 1987). We interpret this in terms of Fig. 5. On initial mixing in salt there are few disordered regions in xanthan suitable for junction-zone formation, and such junction-zone formation is insufficient for crosslinking to form a solid gel. The limited junction-zone formation produces gel islands only. On heating above T_c,

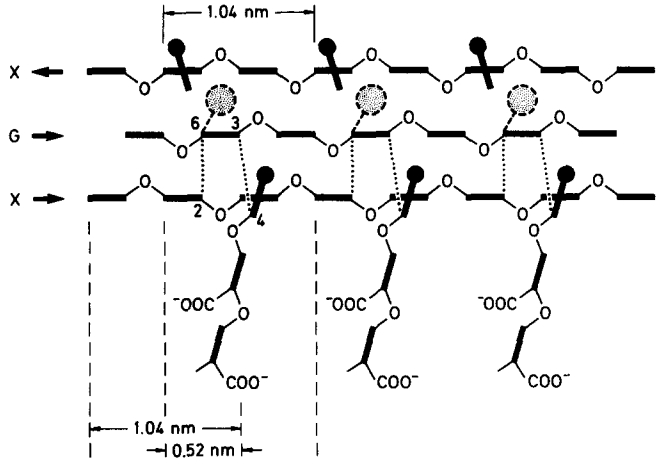

Fig. 5. Model for a xanthan/LBG junction zone. X — xanthan chain; G — LBG chain. Arrows show directionally from non-reducing ends. The backbone conformation for each chain is the flat ribbon. The side chains of the upper xanthan molecule are on the back edge, and are shown only in part. Possible hydrogen bonds between xanthan and LBG, based on space-filling, molecular model building, are shown. Broken, dotted circles show possible positions of 6-*O*-α-D-galactopyranosyl units on the rear edge of the LBG chain.

essentially all the xanthan is converted to the disordered form, and cooling in the presence of LBG provides the optimal conditions for junction-zone formation to occur. This could include the chain directionality such as that proposed in Fig. 5. If such a chain directionality is essential, it could contribute to limiting the size and the number of junction zones. Either unsubstituted mannan sequences or sequences with only one edge substituted are 'allowed' to form junction zones. If a region of the mannan backbone with a particular edge substituted is followed by one with the opposite edge substituted, it would cause termination of a jucntion zone involving that particular xanthan chain. The 'new' unsubstituted edge could commence a new junction zone with another xanthan chain, but this would probably occur some distance away from the initial junction-zone region.

ACKNOWLEDGMENTS

This project was supported by funds from the Australian Research Council. We thank Mr Martin Dudman for drawing the diagrams and those of our earlier publications.

REFERENCES

Cairns, P., Miles, M. J. & Morris, V. J. (1986). *Nature (London)*, **322**, 89.
Cairns, P., Miles, M. J., Morris, V. J. & Brownsey, G. J. (1987). *Carbohydr. Res.*, **160**, 410.
Cheetham, N. W. H. & Mashimba, E. N. M. (1988). *Carbohydr. Polym.*, **9**, 195.
Cheetham, N. W. H. & Punruckvong, A. (1985). *Carbohyr. Polym.*, **5**, 399.
Cheetham, N. W. H. & Punruckvong, A. (1989). *Carbohydr. Polym.*, **10**, 129.
Cheetham, N. W. H., McCleary, B. V., Teng, G., Lum, F. & Maryanto (1986). *Carbohydr. Polym.*, **6**, 257.
Dea, I. C. M., Morris, E. R., Rees, D. A., Welsh, E. J., Barnes, H. A. & Price, J. (1977). *Carbohydr. Res.*, **57**, 249.
Dubois, M., Gilles, K. A., Hamilton, J. K., Rebers, P. A. & Smith, F. (1956). *J. Amer. Chem. Soc.*, **28**, 350.
Frangou, S. A., Morris, E. R., Rees, D. A., Richardson, R. K. & Ross-Murphy, S. B. (1982). *J. Polym. Sci. Polym. Lett.*, **20**, 531.
Lecourtier, J., Chauveteau, G. & Muller, G. (1986). *Int. J. Biol. Macromol.*, **8**, 306.
Milas, M. & Rinaudo, M. (1986). *Carbohydr. Res.*, **158**, 191.
Moorhouse, R., Walkinshaw, M. D. & Arnott, S. (1977). In *Extracellular Microbial Polysaccharides*, ed. P. Sandford & A. Laskin. ACS Symp. Ser. 45, American Chemical Society, WA, DC, USA, p. 90.

Morris, E. R., Rees, D. A., Young, G., Walkinshaw, M. D. & Darke, A. (1977). *J. Mol. Biol.*, **110**, 1.
Norton, I. T., Goodall, D. A., Frangou, S. A., Morris, E. R. & Rees, D. A. (1984). *J. Mol. Biol.*, **175**, 371.
Richardson, R. K. & Ross-Murphy, S. B. (1987). *Int. J. Biol. Macromol.*, **9**, 257.
Smith, I. H., Symes, K. C., Lawson, C. J. & Morris, E. R. (1981). *Int. J. Biol. Macromol.*, **3**, 129.